

UNCLASSIFIED

AD NUMBER: AD0837179

LIMITATION CHANGES

TO:

Approved for public release; distribution is unlimited.

FROM:

Distribution authorized to US Government Agencies and their Contractors; Export Control; 1 Jun 1968. Other requests shall be referred to Space and Missile Systems Organization, Los Angeles AFS, CA 90045.

AUTHORITY

SAMSO ltr dtd 28 Feb 1972

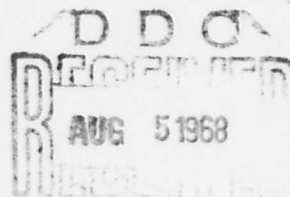
AD837179

RF Bridge Electrical Conductivity Gauge for RMP-B Vehicle

JUNE 1968

Prepared by PLASMA DIAGNOSTICS and MHD DEPARTMENT
Plasma Research Laboratory
Laboratory Operations
AEROSPACE CORPORATION

Prepared for SPACE AND MISSILE SYSTEMS ORGANIZATION
AIR FORCE SYSTEMS COMMAND
LOS ANGELES AIR FORCE STATION
Los Angeles, California



AEROSPACE CORPORATION

THIS DOCUMENT IS SUBJECT TO SPECIAL
EXPORT CONTROLS AND EACH TRANSMITTAL
TO FOREIGN GOVERNMENTS OR FOREIGN
NATIONALS MAY BE MADE ONLY WITH PRIOR
APPROVAL OF SAMSO(SMTTA)

46

Air Force Report No.
SAMSO-TR-68-238

Aerospace Report No.
TR-0158(3220-20)-2

RF BRIDGE ELECTRICAL CONDUCTIVITY GAUGE
FOR RMP-B VEHICLE

Prepared by

Plasma Diagnostics and MHD Department
Plasma Research Laboratory

Laboratory Operations
AEROSPACE CORPORATION

June 1968

Prepared for

SPACE AND MISSILE SYSTEMS ORGANIZATION
AIR FORCE SYSTEMS COMMAND
LOS ANGELES AIR FORCE STATION
LOS ANGELES, CALIFORNIA

This document is subject to special export controls
and each transmittal to foreign governments or
foreign nationals may be made only with prior
approval of SAMSO (SMTTA)

FOREWORD

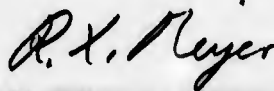
This report is published by the Aerospace Corporation, El Segundo California, under Air Force Contract No. F04695-67-C-0158. The report was authored by the following members of the Plasma Diagnostics and MHD Department:

D. A. McPherson
O. L. Gibb
W. B. Harbridge

and A. E. Fuhs, Consultant to the Plasma Research Laboratory and Professor of Aeronautical Engineering at the Naval Postgraduate School, Monterey, California. The authors would like to thank W. B. Grabowsky, who provided the HCl test solutions for the thick calibrated-conductivity samples, and E. A. Fives, who did much of the construction and testing of the flight instruments.

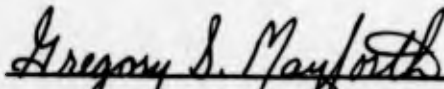
This report, which documents research carried out from August 1967 through February 1968, was submitted on 8 May 1968 to Lt. Gregory S. Mayforth for review and approval.

Information in this report is embargoed under the Department of State International Traffic In Arms Regulations. This report may be released to foreign governments by departments or agencies of the U. S. Government subject to approval of SAMSO, or higher authority within the Department of the Air Force. Private individuals or firms require a Department of State export licence.



R. X. Meyer, Director
Plasma Research Laboratory

Publication of this report does not constitute Air Force approval of the report's findings or conclusions. It is published only for the exchange and stimulation of ideas.



Gregory S. Mayforth, Lt. USAF
Project Officer

ABSTRACT

The Reentry Measurements Instrument Package (RMIP) on the Reentry Measurements Vehicle (RMV) is designed to measure properties of the boundary layer and wake for a sharp nosed, slender body. One of the experimental instruments is an rf bridge that measures the dc conductivity of the plasma sheath formed about the vehicle. Because conductivity is directly proportional to electron density, knowledge of the electron-neutral collision frequency is sufficient to determine the electron density from the conductivity. For the RMP-B vehicle, it is expected that the conductivity will be in the range 0.3 to 1.0 mho/m for a refrasil heat shield with 50 ppm Na or equivalent contaminants. The conductivity meter was designed with a dynamic range of 0.1 to 10.0 mho/m. The system study providing design criteria is reviewed. Detailed operational information on instrument performance is presented.

CONTENTS

FOREWORD	ii
ABSTRACT	iii
NOMENCLATURE	vii
I. INTRODUCTION	1
II. OPERATING PRINCIPLES	3
III. DESIGN PARAMETERS	7
IV. SYSTEM DESCRIPTION	13
A. Power System	13
B. Coil	15
C. Bridge	16
D. Thermal Compensation	20
E. RF Preamplifier, Filter, and Amplifier	21
F. Phase-Sensitive Demodulator	24
G. Telemetry Outputs	24
V. SYSTEM CALIBRATION AND PERFORMANCE	29
REFERENCES	39

FIGURES

1.	Block Diagram of RF Bridge Conductance Gauge.	4
2.	Estimated Electrical Conductivity and Typical Trajectories for a Sharp Cone	8
3.	Power System Schematic	14
4.	RF Bridge Schematic	17
5.	Simplified RF Bridge Schematic	18
6.	Double Coil Configuration	22
7.	RF Preamplifier, Filter, and Amplifier Schematic	23
8.	Phase Sensitive Demodulator Schematic	25
9.	Telemetry Output Circuits	28
10.	Calibration Data for High-Gain Channel	31
11.	Calibration Data for Low-Gain Channel	31
12.	Recording of High- and Low-Gain Channels During Application and Removal of 0.025 mho Test Fixture	32
13.	Geometrical Factor $W(z')$ vs Normalized Axial Separation z	34
14.	Instrument Gain vs RF-Amplifier-Output-Monitor Reference Voltage	36
15.	Temperature-Monitor Voltage vs Temperature	37

NOMENCLATURE

a	coil-face/boundary-layer separation (in.)
e	bridge drive voltage (V)
Δe	bridge signal voltage (V)
$f(z)$	profile of conductivity in boundary layer
n	electron density (cm^{-3} or m^{-3})
N	number of turns of field coil
r_c	field coil radius (m)
$W(z)$	instrument response as a function of axial separation z
Z_1, Z_2, Z_3, Z_4	bridge impedances
z	axial distance from field-coil face (in.)
z', δ', a'	dimensions z, δ, a , normalized to unity at r_c
δ	boundary layer thickness (in.)
ϵ	permittivity of vacuum = $10^{-9}/36\pi$ (F/m)
μ	permeability of vacuum = $4\pi \times 10^{-7}$ (H/m)
ν	electron-neutral collision frequency (sec^{-1})
σ_0	peak conductivity in boundary layer (mho/m)
σd	product of conductivity and thickness for sample of uniform conductivity (mho)
ω	bridge frequency (rad/sec)
ω_p	plasma frequency (rad/sec)

I. INTRODUCTION

The purpose of the Reentry Measurements Instrument Package (RMIP) on the Reentry Measurements Vehicle (RMV) is to measure physical properties of the boundary layer and wake for a sharp nosed, slender body. The conductivity gauge measures the dc electrical conductivity in the boundary layer by means of an rf bridge technique. In all, six RMV's will be equipped with conductivity meters.

Much of the design study pertinent to establishing the specifications for the flight instrument has been published previously. In Section III these results will be summarized and discussed along with other specifications imposed by the RMV. Section II contains the operating principles. The details of circuit design are in Section IV. The engineering information of Section IV is included for completeness. The calibration procedures are discussed and compared in Section V. This section includes data on sensitivity and stability.

BLANK PAGE

II. OPERATING PRINCIPLES

The conductivity gauge is shown in block diagram form in Fig. 1. The subsystems are power supply, rf oscillator and driver, rf bridge, rf detector and amplifier, phase-sensitive demodulator, and differential signal telemetry conditioners.

The power supply is a dc-dc converter. This type permits the isolation of power ground from signal ground and provides ± 15 V for the integrated circuits.

The signal detection function of the instrument is fulfilled by the rf bridge. The remainder of the circuitry is used for signal discrimination and conditioning. One leg of the bridge consists of a 80-turn 4-in. -diam coil, mounted at the inner surface of the reentry-vehicle heat shield. The bridge is driven with a 300-kHz oscillator. The fringing magnetic field of the coil is about 0.03 G at the outer surface of the heat shield.

During reentry, this oscillating magnetic field induces currents in the plasma layer formed about the R/V. The induced currents form a secondary circuit, and the impedance of the driving coil is altered. Dissipation caused by the finite conductivity of the plasma introduces a resistive component in the coil impedance, and this resistive component gives rise to the signal.

The impedance variation is detected as a variation in bridge signal voltage. The bridge signal voltage preamplifier is an operational amplifier used in a differential configuration.

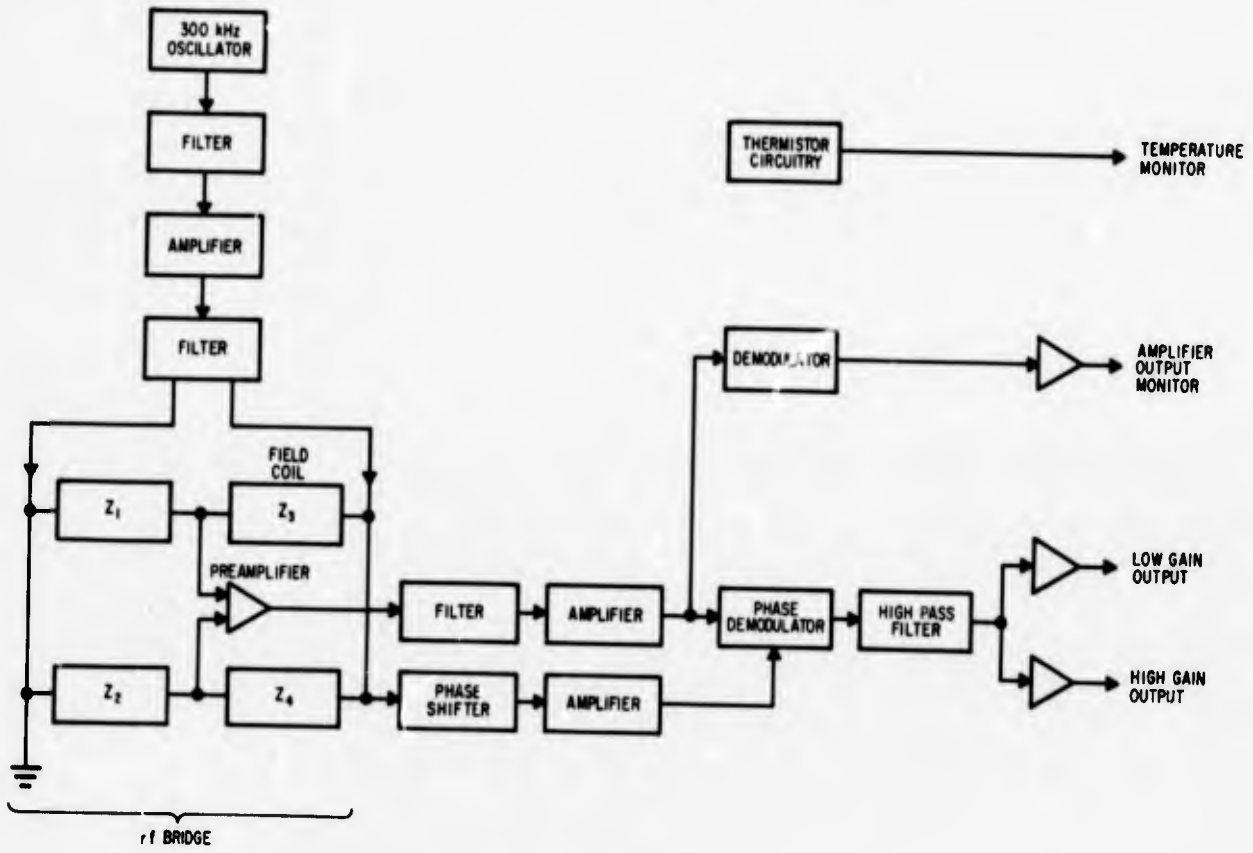


Fig. 1. Block Diagram of RF Conductivity Gauge

After filtering and amplification, the bridge output is phase demodulated. The phase of the signal voltage selected for demodulation is 90 deg out of phase with the rf bridge drive voltage. This discriminates against the reactive part of the impedance change. The output of the phase demodulator is a dc voltage representing the resistive part of the impedance change.

Before the remainder of the instrument operation is described, a preliminary consideration of sensitivity is necessary. A complete analysis of signal levels and instrument sensitivity is presented in Section III. For the RMP-B vehicle, it is expected that, during reentry, the induced coil-impedance variation will be approximately one part in 10^5 .

It is impossible to maintain the bridge balance to this degree of accuracy because of component dependence upon temperature and other environmental conditions. This limitation is overcome by subtracting from the signal output the quiescent out-of-balance voltage existing prior to reentry.

The phase demodulator output is filtered by a high-pass network with a 24-sec RC time constant. The quiescent out-of-balance voltage is slowly varying compared to the expected signal and is attenuated by the high-pass filter. The signal will consist of components with frequencies far greater than 0.0068 Hz, the -6 dB point of the filter.

The data recording period during reentry will be approximately 10 sec. With a 24-sec RC time constant and a sufficiently high telemetry sample rate, it is possible to integrate the telemetry data and obtain the variations in detector voltage during reentry.

With this differential feature, the bridge balance must be maintained to one part in 10^3 , which is not simple but is possible. This limitation is required so that the rf signal voltage amplifier does not saturate. It may also be noted that the system remains linear if the bridge is balanced to this degree of accuracy.

There are high- and low-gain output channels to provide a dynamic range of 40 dB. The high-gain channel represents signal levels of $\sigma d = 0.002$ to 0.02 mho, where σd is the product of conductivity and boundary-layer thickness. The low-gain channel is approximately ten times less sensitive.

In addition to the high- and low-gain telemetry channels, which are sampled at a rate of 127/sec, there are two low-rate channels. One of these is used to monitor the out-of-balance voltage to ascertain whether the rf amplifier is saturated. The other channel is used to monitor the temperature of the coil.

III. DESIGN PARAMETERS

The design of the instrument is based upon a study reported previously by Fuhs, et al. (Ref. 1). This work used data presented by Dix pertaining to plasma parameters around a conical reentry vehicle (Ref. 2). The most significant results of these studies for the instrument design are the values of conductivity and boundary layer thickness vs R/V altitude and speed. Recent data do not significantly alter the results of these studies (Ref. 3).

The electrical conductivity σ can be defined in terms of the electron-neutral collision frequency ν and the electron density n as $\sigma = ne^2/m\nu$ (Ref. 4). With the expression for plasma frequency $\omega_p^2 = ne^2/m\epsilon_0$, the conductivity can be written $\sigma = \omega_p^2 \epsilon_0 / \nu$.

Dix's calculations are for a vehicle semivertex angle of 10 deg. The RMP-B vehicle semivertex angle is 8 deg, but the plasma and collision frequencies are not very sensitive to either semivertex angle or distance from the cone vertex. Therefore it will be assumed that the 10-deg semivertex-angle data are applicable.

Isocontours of ν and ω_p vs altitude and velocity are provided by Dix. These data have been converted by Fuhs into isocontours of electrical conductivity vs altitude and velocity, which are reproduced in Fig. 2. In addition, typical trajectories for a range of the ballistic parameter $W/C_D A$ are included.

From Fig. 2, it can be seen that the expected range of conductivity will be on the order of 0.1 to 1.0 mho/m for a typical $W/C_D A$ parameter of 1000.

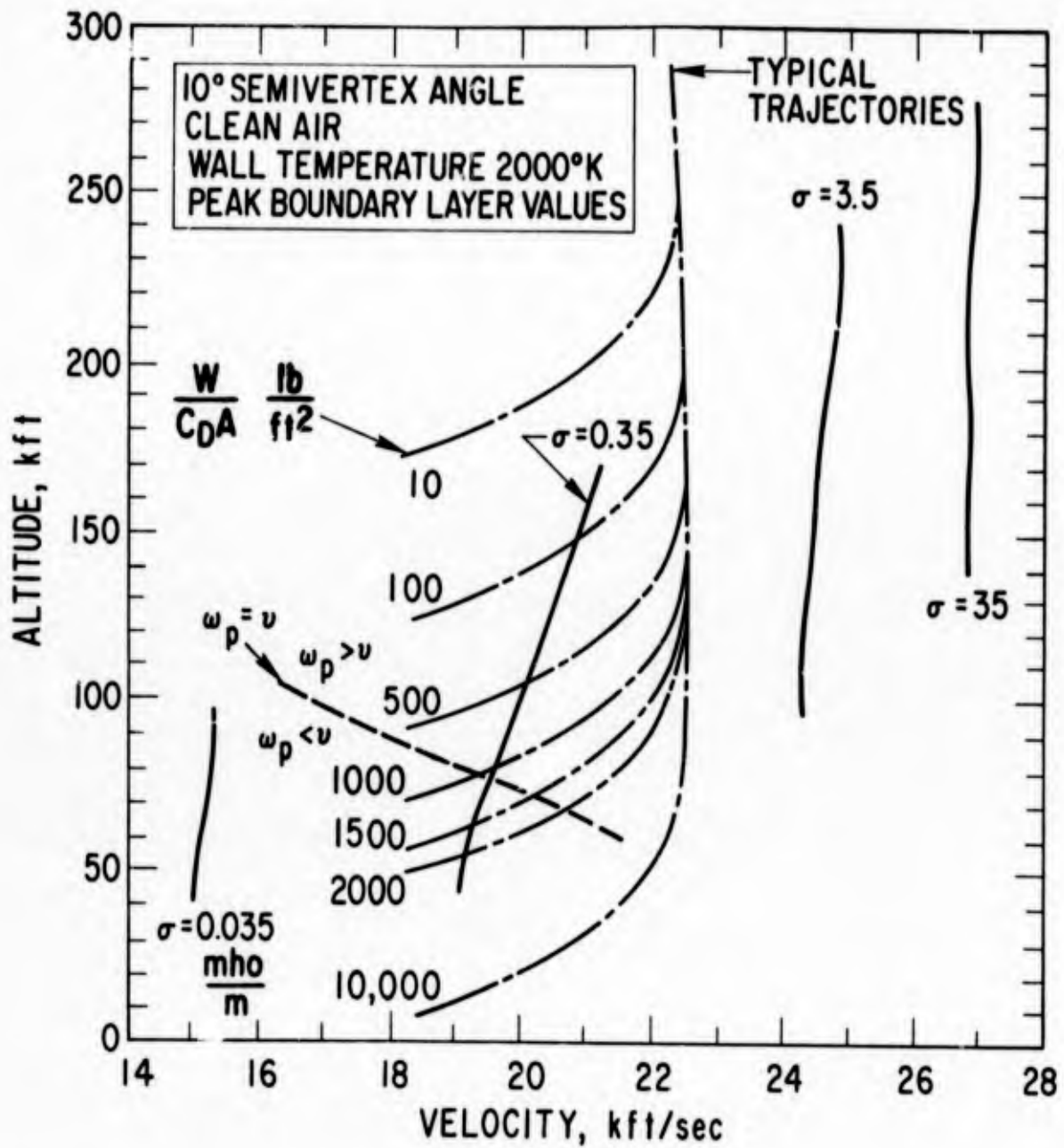


Fig. 2. Estimated Electrical Conductivity and Typical Trajectories for a Sharp Cone (after Ref. 1)

The other significant plasma property to be determined is the sheath thickness. According to Dix, the thickness is insensitive to velocity. From Fig. 5 of Dix (Ref. 2), for a 9-ft separation from the cone vertex, the turbulent boundary layer thickness is approximately 0.7 in. at 100 kft and decreases to 0.4 in. at 50 kft.

In summary, typical electrical conductivities of 0.3 mho/m and sheath thicknesses of 0.5 in. are expected near 100 kft altitude. With these parameters, the effect of the plasma sheath on the rf bridge balance can be evaluated.

The ratio between the change in bridge voltage Δe and the bridge driving voltage e is given by Fuhs as

$$\frac{|\Delta e|}{|e|} = \sigma_0 \left[2\pi \left(\frac{\mu\omega N}{\pi} \right)^2 r_c^3 \frac{|Z_2|}{|Z_1 + Z_4|^2} \right] \int_{a'}^{\infty} W(z') f(z') dz' \quad (1)$$

To obtain this expression, it is assumed that the coil is of short axial length. The integral accounts for geometrical factors such as the spatial dependence of the magnetic field and the profile of the conductivity in the sheath. The conductivity is assumed to have the form $\sigma_0 f(z)$. The axial separation $z' = z/r_c$ is then normalized to the coil radius r_c . As mentioned previously, the conductivity is not a function of distance from the cone vertex.

The spatial variation of the magnetic field is provided by the function (Ref. 5)

$$W(z') = \int_0^{\infty} \frac{1}{k^2} \left[\left(1 - \frac{1}{2} k^2 \right) K - E \right]^2 dr' \quad (2)$$

The K and E are complete elliptic integrals of the first and second kind (Ref. 6). The function $k^2 = 4 r_c r / [(r_c + r)^2 + z^2]$ can be expressed in dimensionless units $r' = r/r_c$ and $z' = z/r_c$. Therefore $W(z')$ is independent of coil radius r_c .

It is desirable to maximize the ratio $\Delta e/e$ to obtain the highest possible signal-to-noise ratio. The disposition of the impedances Z_1 , Z_2 , Z_3 , and Z_4 can be seen in Fig. 1. Maximum signal is obtained when $Z_1 \sim Z_2 \sim Z_3 \sim Z_4$. Thus the ratio $|Z_2|/(Z_1 + Z_4)^2$ is proportional to $1/\omega L$, where L is the inductance of the coil.

According to Grover (Ref. 7, Eq. 100), the inductance of the coil varies linearly with $N^2 r_c$. Thus, in Eq. (1), the function $\omega^2 N^2 r_c^3 |Z_2|/|Z_1 + Z_4|^2$ varies as $\omega^2 N^2 r_c^2 / \omega N^2 r_c = \omega r_c^2$.

To some extent, the signal is independent of the number of turns N in the coil. However, if N is too large, the distributive capacity of the coil shunts the current from turn to turn and decreases the magnetic field. If the turns are too few, the impedances Z_1 , Z_2 , and Z_4 are so small as to be intractable. Also, distributed capacity in leads becomes significant, and the input impedance to the bridge loads down the bridge oscillator-driver. Therefore, the number of turns is selected to provide a bridge input impedance of several $K\Omega$ while maintaining the coil resonant frequency at least a factor of three greater than the driving frequency.

The most effective parameters to vary are the frequency ω and the coil radius r_c . Not only does r_c occur to the second power, but the lower

power limit on the integral over z' decreases with increasing r_c . The coil radius is restricted to a maximum of 4 in. on the RMP-B vehicle. The maximum limit on the frequency is imposed by the restriction that the driving frequency be maintained below the coil resonant frequency. The resonant frequency can be increased by decreasing the number of turns, but this too has a limit because it reduces the input impedance of the bridge. For the configuration discussed here, the maximum frequency possible is around 1 MHz. The operating frequency of the first flight instruments was arbitrarily selected at 300 kHz. Table I summarizes the design parameters required in Eq. (1) to determine the $\Delta e/e$. With these values, a value of $\Delta e/e \sim 10^{-5}$ is obtained.

Table I. RF Bridge Conductivity Gauge Design Parameters.

Parameter	Symbol	Value
Coil turns	N	80
Coil radius	r_c	2 in.
Coil/boundary-layer separation	a	0.5 in.
Spatial peak conductivity	σ_0	0.3 mho/m
Frequency	$\omega/2\pi$	300 kHz
Boundary layer sheath thickness	δ	0.5 in.
Bridge impedance	Z	2 k Ω each leg
Geometrical factor ^a	$\int_{a'}^{a'+\delta'} W(z')f(z')dz'$	0.06

^aAfter Fuhs (Ref. 1, Fig. 8), $f(z)$ assumed to be $\sin[\pi(z'/\delta' - a'/\delta')]$.

BLANK PAGE

IV. SYSTEM DESCRIPTION

In this section, pertinent engineering information is provided. These details are not required to understand the operation of the instrument, but rather provide the basic groundwork for future development.

A. POWER SYSTEM

The requirements on the power supply are to provide regulated voltages of ± 15 and $+22$ Vdc and to separate the power return from the output signal ground. The signal ground is chassis ground, whereas the power return is separated from the chassis ground. The instrument uses 150 mA from the unregulated 28-V RMIP bus.

To satisfy these criteria, a dc-dc converter is used as shown in Fig. 3. The output of the converter consists of a transformer with a common primary and two center-tapped secondaries. The outputs of the secondary windings are full-wave demodulated with opposite polarities. This provides ± 24 Vdc isolated from the power input. These plus and minus voltages are inputs to series regulators providing regulated ± 15 Vdc supplies for the integrated circuits.

Each circuit board in the instrument has a 22-V series regulator operated from the +24-V demodulator. This isolates various sections of the instrument that use +22 V.

All voltages and ground lines from the power supply board pass through LC T-filters to attenuate rf generated by switching transients in the dc-dc converter.

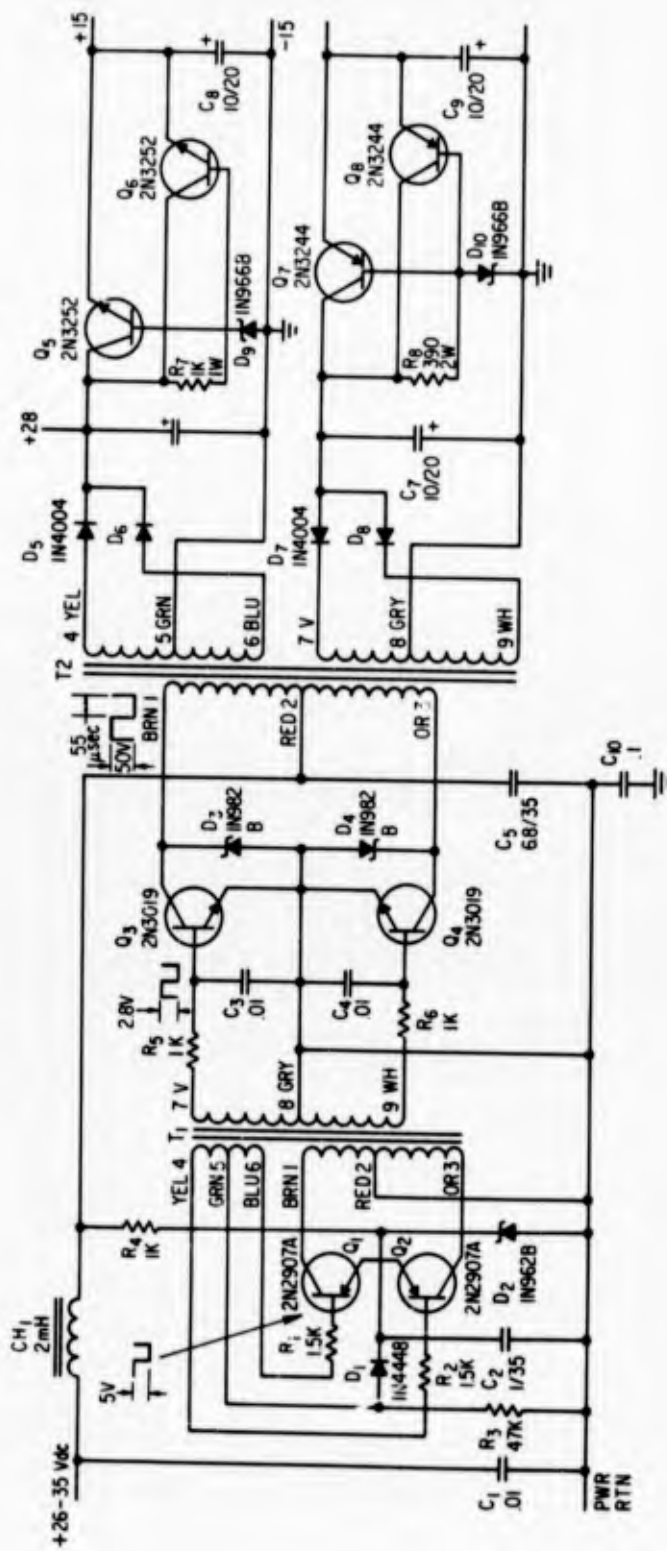


Fig. 3. Power System Schematic

B. COIL

The coil that generates the magnetic field in the boundary layer is one leg of the rf bridge. Table II summarizes the coil electrical properties.

Table II. Coil Electrical Properties

Parameter	Value	Remarks
R, measd	190 Ω	In ferrite cup
L, measd	1.08 mH	In ferrite cup
Q	0.034	In ferrite cup
L, measd	0.70 mH	No ferrite cup
L, calcd	0.62 mH	Thick coil formula, no ferrite
Impedance, measd	2.17 k Ω	At 300 kHz
Impedance, calcd	2.04 k Ω	At 300 kHz

The measured and calculated inductances are within 11% of each other. The coil formula used (Ref. 7) was for small axial length. This agreement justifies the assumption mentioned in Section III regarding integrations along the axial direction.

The purpose of the ferrite cup is to reduce the number of flux lines passing through the metallic structure of the instrument package. Any motion of this structure relative to the coil induces spurious signals. The ferrite lowers the fringing field sufficiently so that this effect is small.

The face of the coil is vapor plated with 10^{-6} -in. aluminum. This coating is electrically connected to the coil housing to provide an integral electrostatic shield. This stabilizes the distributive capacitance.

C. BRIDGE

Figure 4 is the schematic diagram of the rf bridge and preamplifiers. The biasing network for the Q85AH integrated amplifier is standard and not shown. The bridge and preamplifier are housed in a module separate from the remainder of the circuitry. The purpose of this is to minimize and stabilize distributive capacity.

The leads to the driving coil are RG 196 coaxial cables with shield grounded both at the coil and the bridge. This technique provides a lead capacitance sufficiently independent of lead movement or position.

Figure 5 is a simplified version of the bridge that can be used to explain the balancing procedure and the requirements for refinements evident in Fig. 4.

The condition for bridge balance in Fig. 5 is

$$\frac{Z_3}{Z_1 + R_1} = \frac{R_4}{R_2 + R_5}$$

The impedances Z_1 and Z_3 are complex, but the ratio $Z_3/(Z_1 + R_1)$ must be real. The impedance Z_1 is a 1-mH Collins inductor, with a 2.4- Ω resistance. Thus $\text{Re } Z_3/\text{Re } Z_1 = 75$, and R_1 can be increased to make $Z_3/(Z_1 + R_1)$ real. The magnitudes of the two ratios can be equated by adjusting R_5 .

In summary, R_1 is used to adjust for phase balance and R_5 is used to adjust for impedance balance.

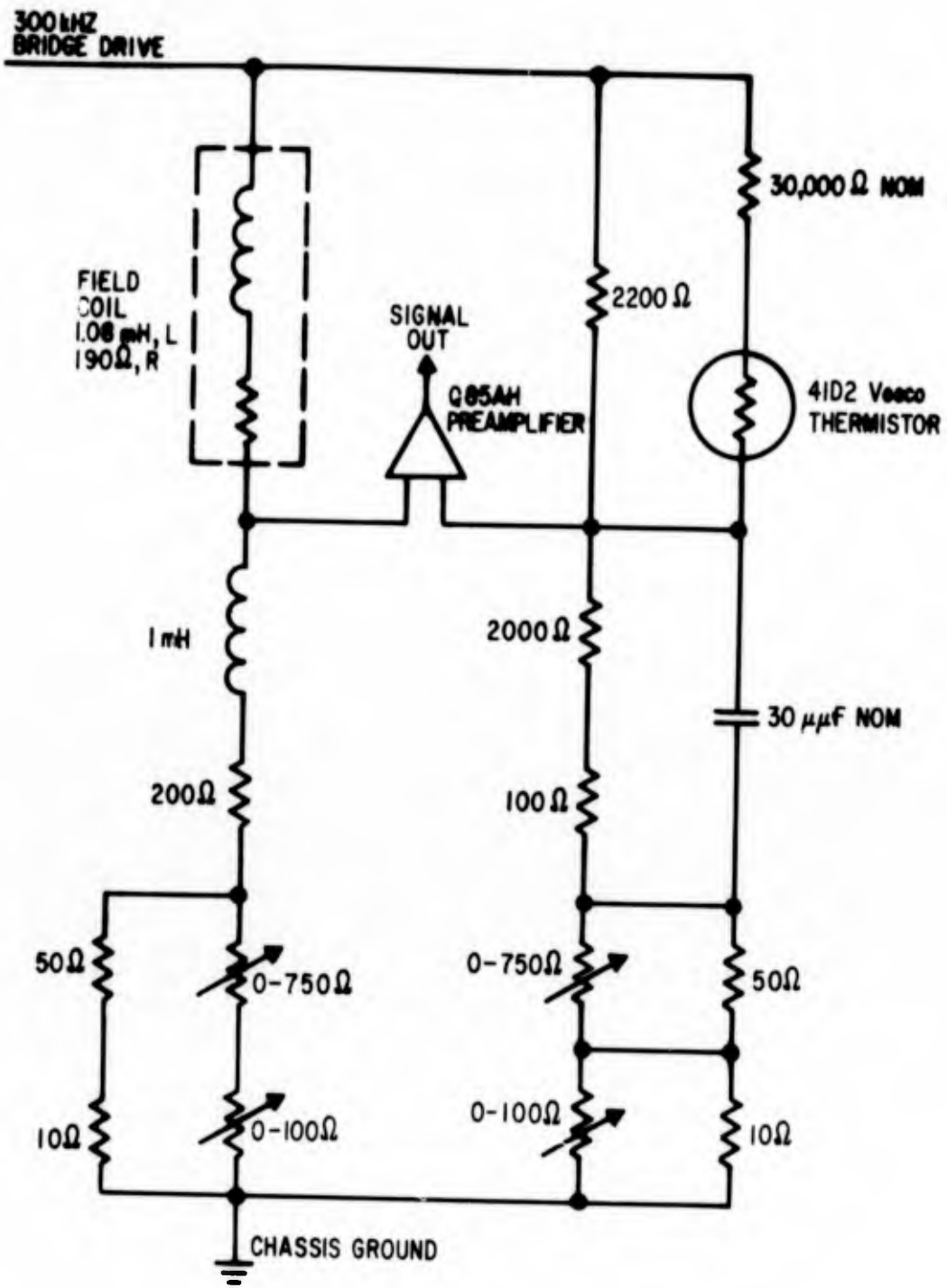


Fig. 4. RF Bridge Schematic

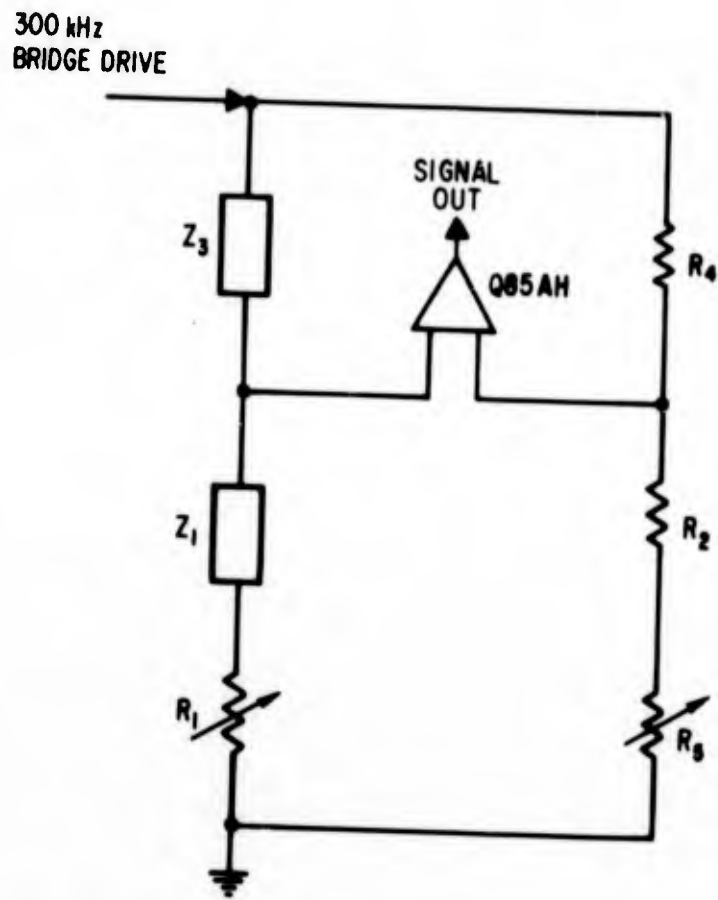


Fig. 5. Simplified RF Bridge Schematic

The refinements required for an operational bridge are as follows. Because the bridge must be balanced to one part in 10^3 , the resolution of the adjustment in R_2 and R_5 must be on the order of $1\ \Omega$. To obtain this resolution and to have sufficient range, the actual bridge has series-parallel combinations of resistors and potentiometers. The $250\text{-}\Omega$ potentiometers provide a coarse adjustment and the $100\text{-}\Omega$ potentiometers provide a fine adjustment.

The distributive capacitance in the bridge introduces a capacitive reactive component to the resistive legs. This is compensated by a small capacitor across R. The distributed capacitance of this particular instrument requires that the compensation be across R_2 .

The other difference between the actual bridge circuit and the simplified one is the resistor-thermistor series combinations in the Z_4 leg. This is included to provide thermal compensation for the impedance variation with temperature of the components in the bridge circuit.

The bridge is driven by 300-kHz crystal-controlled oscillator. The temperature coefficient of frequency $\Delta f/f$ is less than 10^{-4} from 0°C to 85°C . The oscillator output is filtered and amplified as shown in Fig. 1. Each bandpass filter has -6 dB attenuation at the fundamental frequency, and -40 dB at the second harmonic. The overall gain between the oscillator and the bridge is +10 dB, which provides a 2-V rms driving voltage across the bridge. An impedance change is one part in 10^5 causes a $10\ \mu\text{V}$ rms signal at the bridge output. This is the expected signal level for the RMP-B vehicle.

D. THERMAL COMPENSATION

The major difficulty with the instrument is the temperature variation of component impedances in the bridge. Table III is a list of component impedances and the estimated temperature effect.

Table III. Component Impedances and Estimated Temperature Effect

Component	Impedance, k Ω	Temperature Coefficient	Impedance Temperature- Effect Variation, $\Omega/^{\circ}\text{C}$
Coil, inductance	2	10^{-4}	+0.2
Coil, resistance	0.200	$<10^{-6}$	+0.0002
1-mH MIH inductor	2	$\pm 2 \times 10^{-5}$	± 0.04
Distributed capaci- tance	14 (shunt)	-2×10^{-4}	-0.006
Bridge resistors, metal film	2	$<10^{-6}$	+0.002
Potentiometers	30	-5×10^{-4}	< -0.02

The large impedance variation of the coil inductance is caused by the 0.03% temperature coefficient of the ferrite permeability. The effect of the stray capacitance is a crude estimate. It was assumed that the capacitance varies inversely with linear thermal expansion. The magnitude of the capacitance was assumed to be that required in the Z_2 leg.

In the first instrument, temperature compensation was attempted by placing thermistors in the bridge circuit as shown in Fig. 4. This technique worked on breadboard models but was not as effective in the flight configuration. When the circuitry is packaged, sufficient heat is generated to upset the balance by heating one element more than another.

A second technique consists of replacing the 1-mH coil in Z_1 by a coil nearly identical to the driving coil in Z_3 . This alleviates the temperature stability problem. Figure 6 is a photograph of this configuration, which is used in all but the S/N 001 and qualification instruments. The ballast coil Z_1 is shown in the instrument housing. The field coil and ferrite cup are shown above the housing.

E. RF PREAMPLIFIER, FILTER, AND AMPLIFIER

Figure 7 is a schematic of the rf preamplifier, filter, and amplifier. The overall gain of this subsystem is 5000. This provides a 50-mV rms signal for a change of bridge balance of one part in 10^5 .

The Philbrick Q85AH operational amplifier is well suited for the preamplifier in the differential configuration. The small size and 100-k Ω input impedance combine to provide no significant loading of the bridge.

The bandpass filter and amplifier are the same as used to amplify the 300-kHz oscillator output. There is no filter at the output of the amplifier because the phase-sensitive demodulator acts as an extremely sharp bandpass filter in addition to selecting the proper phase.

The gain of the rf amplification subsystem was selected to provide a signal level sufficiently greater than the drift of the phase demodulator output, which is on the order of a millivolt. If the gain is too high, then a small unbalance of the bridge will cause the rf amplifier to saturate. With a gain of 5000, the bridge can be unbalanced one part in 2500 before the amplifier saturates.

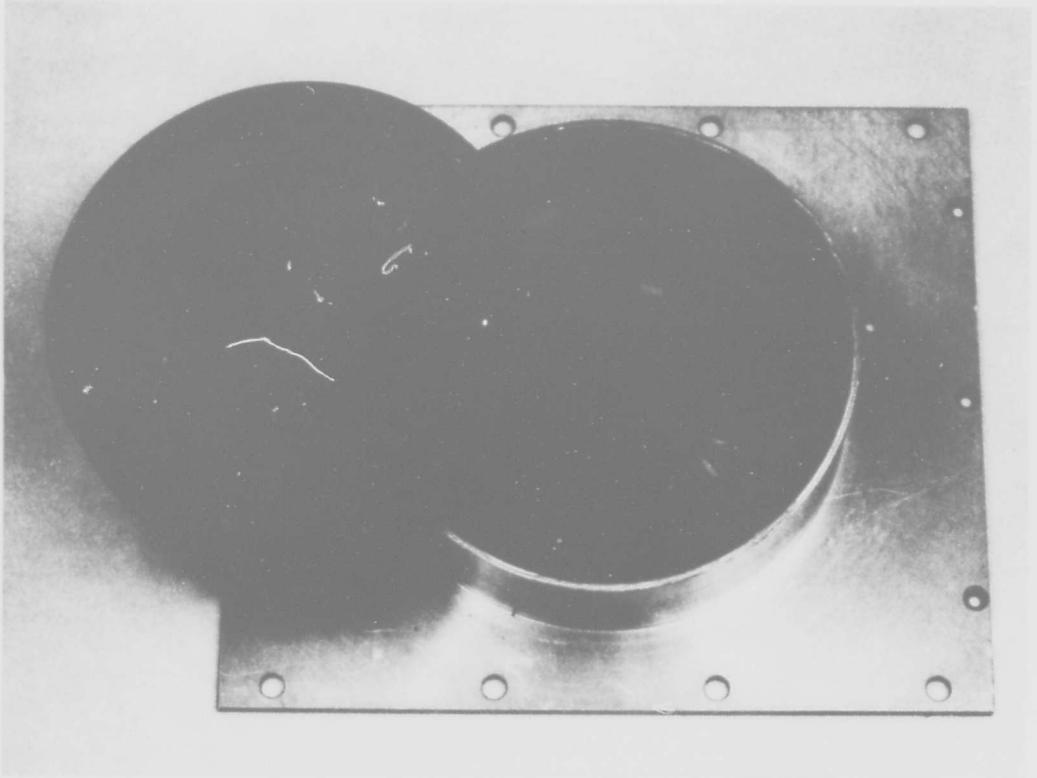


Fig. 6. Double Coil Configuration

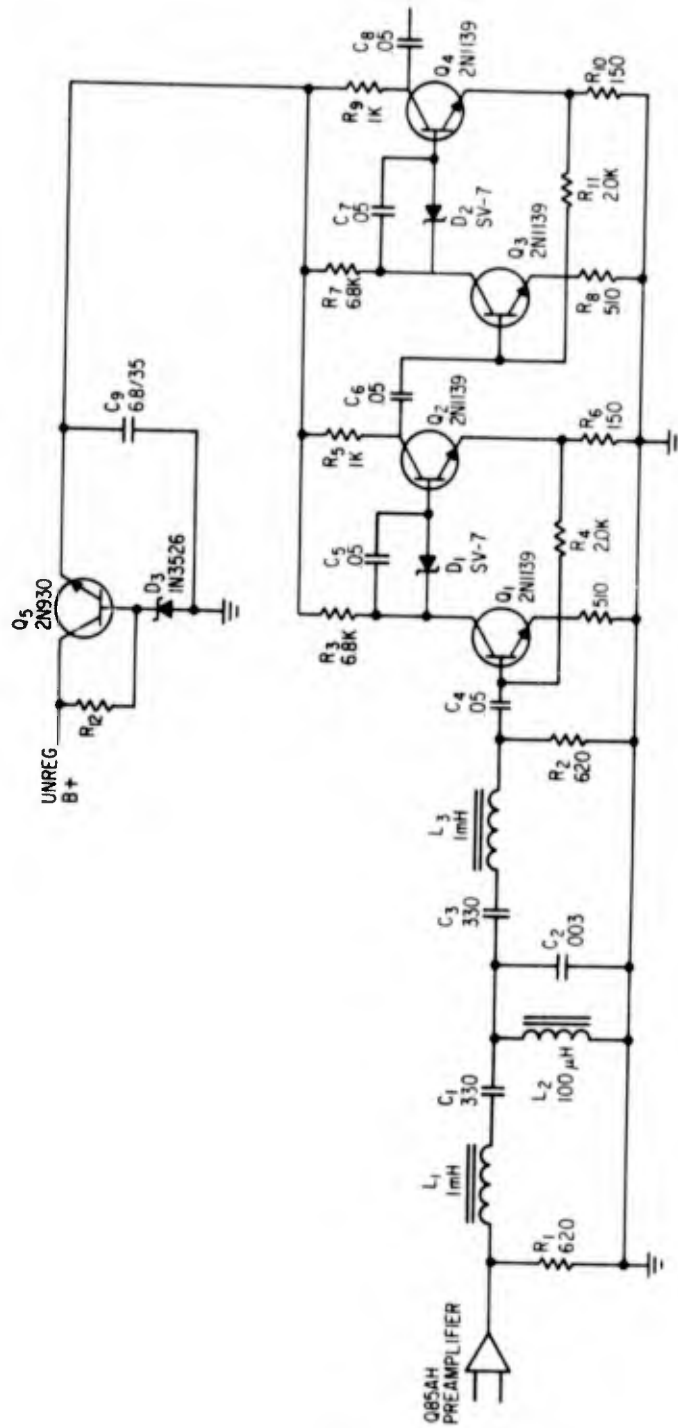


Fig. 7. RF Pre-amplifier, Filter, and Amplifier Schematic

F. PHASE-SENSITIVE DEMODULATOR

The phase-sensitive demodulator selects the proper phase of the rf signal and converts it to a dc voltage. There is -40 dB rejection of any component of incorrect phase or frequency. The desired signal is attenuated by -3 dB.

The demodulator is driven by a signal derived from the 300-kHz voltage applied to the rf bridge. This voltage is passed through a phase-shifting RC network and one stage of amplification. The phase shift is adjusted so that an rf signal caused by a reactive impedance variation is rejected by the demodulator. The amplifier, similar to that in the bridge driver, is required to provide isolation between the rf bridge driving voltage and the demodulator driving voltage.

Figure 8 is a diagram of the phase demodulator and driving voltage circuits.

G. TELEMETRY OUTPUTS

There are four telemetry outputs. Two have a data rate of 127 samples/sec and two operate at 7 samples/sec. The high-data-rate channels are used to telemeter the phase-demodulated bridge signal at different gains. One low-rate channel monitors the level of the rf amplifier output to indicate whether the amplifier is saturated. The other low-rate channel monitors the temperature of the coil.

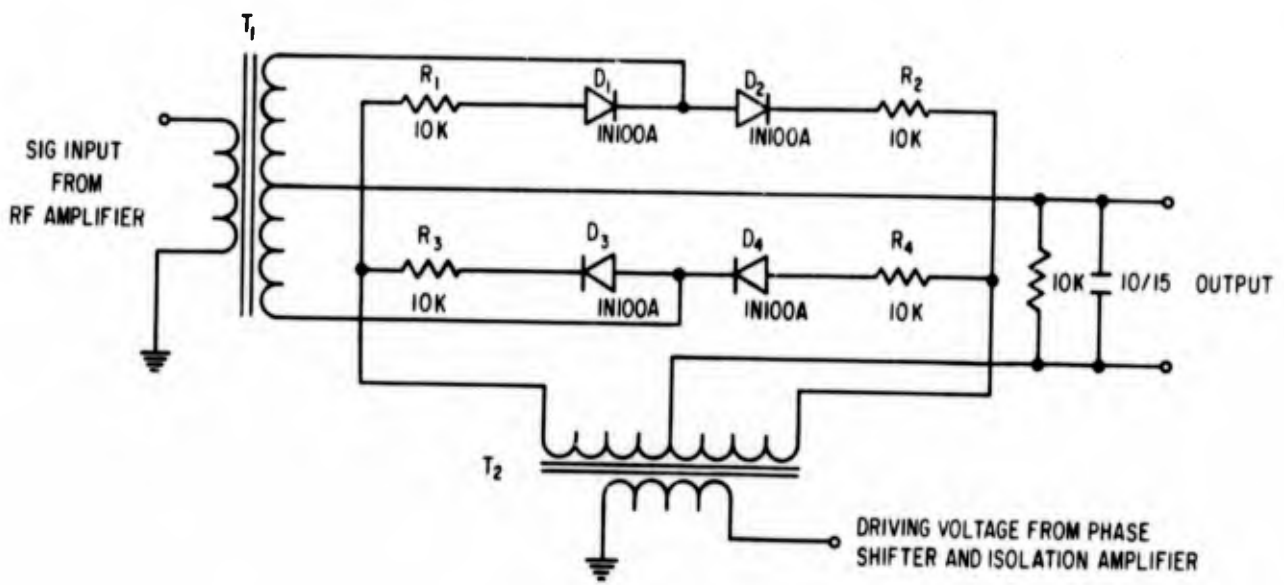


Fig. 8. Phase Sensitive Demodulator Schematic

The telemetry output signals must be in the range 0 to 6 V with an output impedance of 1 k Ω . The telemetry system calibration is valid in the range 0 to 5 V.

The coil temperature is measured with a simple resistor and thermistor series circuit. The thermistor, a Gulten type 27.5 TD1, has a nominal resistance of 850 Ω and temperature coefficient of -4.4%. For a 5000- Ω current-limiting resistor and 15-V supply, the output at 26°C is 1.7 V.

The other subcommutated telemetry channel monitors the demodulated output of the rf amplifier. This dc voltage is amplified by a Philbrick Q25AH amplifier. Originally, this telemetry channel was assigned to another function, which required a high-input-impedance amplifier. Later instruments will have a less sophisticated output stage than the one shown here.

The two high-data-rate channels telemeter the phase-sensitive demodulator output at different gains. The output from the phase demodulator is filtered by a 24-sec RC-time-constant network. This blocks any steady or slowly varying signal from the output amplifiers.

It is impossible to maintain the bridge balance to one part in 10⁵. Generally the bridge is out of balance by several parts in 10⁴. This has the effect of maintaining a slowly varying voltage of a volt or so at the output of the phase demodulator. The high-pass filter attenuates this out-of-balance signal so that the output amplifier is not saturated. The signal during reentry is expected to last 10 to 15 sec and will not be attenuated as severely.

Because the phase of the out-of-balance signal varies, the resulting phase-demodulated voltage may be of either sign. Therefore the telemetry output amplifiers must have a bias of 2.5 V to maintain the signal in the range 0 to 5 V.

As shown in Fig. 9, the input signal to the dc amplifier of the high-gain channel is the voltage across the total resistance in the RC filter. The low-gain channel uses a fraction of this signal. The restrictions that operational amplifiers have $10\text{-M}\Omega$ input impedance and an output bias of 2.5 V preclude any effective gain adjustment. Therefore, different input signal levels are used to attain the desired overall gains for the two output channels. The output impedance of these amplifiers is 275Ω , well below the 1000Ω requirement of the RMIP.

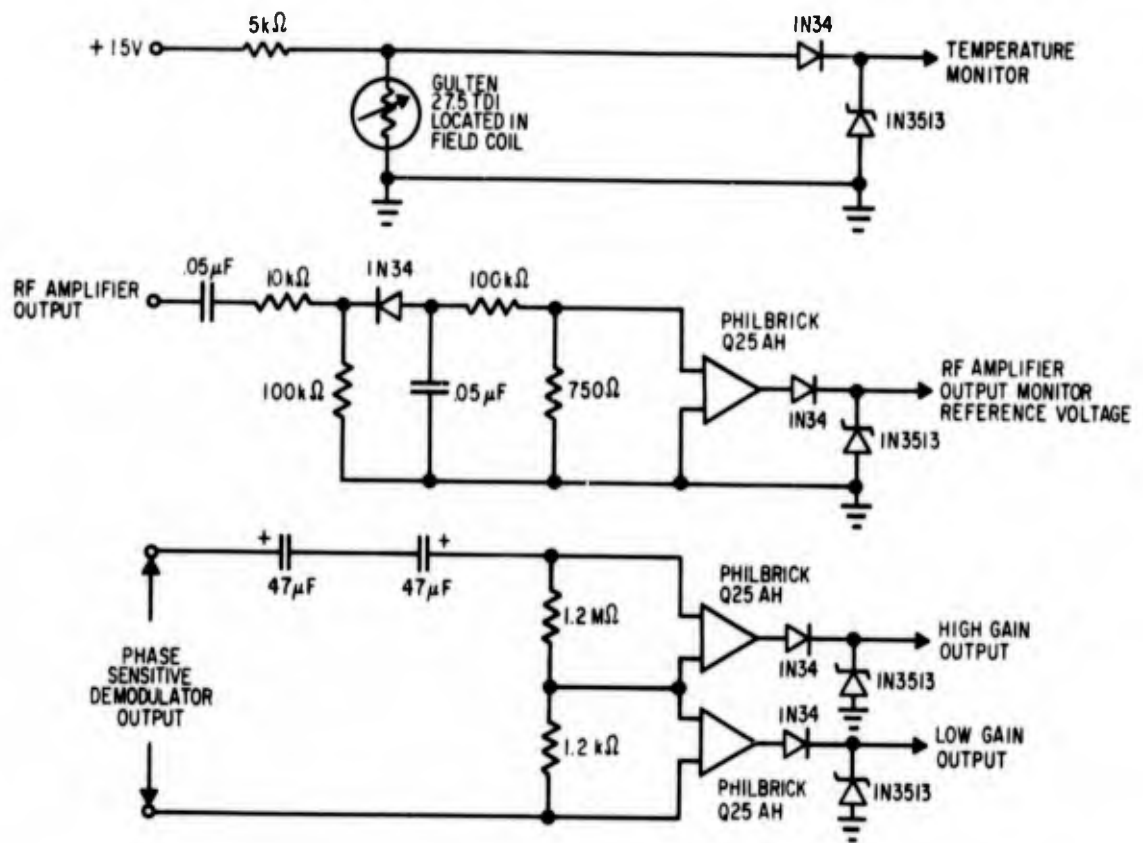


Fig. 9. Telemetry Output Circuits

V. SYSTEM CALIBRATION AND PERFORMANCE

The purpose of the calibration procedure is to determine the sensitivity of the device and the geometrical weighting factor $W(z')$ of Eq. (2) in Section III.

Two types of conducting materials are used for calibration. The most convenient is Eccosorb, a carbonized linear cloth manufactured by Emerson and Cuming, Inc. This material can be obtained in 0.01-in. thickness with nominal resistances of 100, 377, and 1000 Ω /square. Actual resistances vary by 25% and each piece must be individually measured. By using combinations of different samples and several thicknesses, it is possible to construct a series of calibration fixtures with σd parameters of 0.001 mho to 0.1 mho without having the sample exceed 0.1-in. thickness.

Dilute solutions of HCl are used to check the Eccosorb data and to verify the measured weighting factor $W(z')$. These solutions are contained in hollow sections of plexiglas, curved to match the contour of the RMP-B vehicle. Different thicknesses are used to simulate various reentry sheath thicknesses.

To obtain conductivities of 1 mho/m, solutions with less than 1% HCl are required. These weak solutions are susceptible to conductivity variation because of impurities and temperature changes. The stronger the solution, the more stable the conductivity. It is expected that 10-mho/m solutions provide more reliable and reproducible calibration data.

For the instruments on the RMP-B vehicle, solutions of 0.3, 1.7, and 9.1 mho/m are used. The conductivities of these solutions were measured by the Aerospace Aerodynamics and Propulsion Research Laboratory with rf bridge techniques.

Figures 10 and 11 show typical calibration curves of signal output vs the parameter σd for the high- and low-gain channels. Most of these data were obtained from the Eccosorb test fixtures. The resistance of each specimen in Ω/square is the inverse of σd in mhos. These data represent the response to a thin specimen of conducting material located on a curved surface 0.5 in. from the coil face. This separation is equivalent to the thickness of the ablation material on the RMP-B vehicle.

The signal output occurs as a change in telemetry voltage, because of the high-pass filter between the phase demodulator and the output amplifier. Figure 12 is a recording of the high- and low-gain channel outputs while a $\sigma d = 0.025$ -mho test fixture was applied and removed several times. Note the slow decay back to the 2.5-V bias level on both channels after each change.

The actual voltage that would be obtained without the high-pass filter is

$$V(t) = V(t=0) + V_o(t) + \frac{1}{RC} \int_0^t V_o(t') dt' \quad (3)$$

The $V(t = 0)$ is the voltage prior to the perturbation. The recorded voltage is $V_o(t)$, and RC is the time constant of the high-pass filter. The $V(t = 0)$

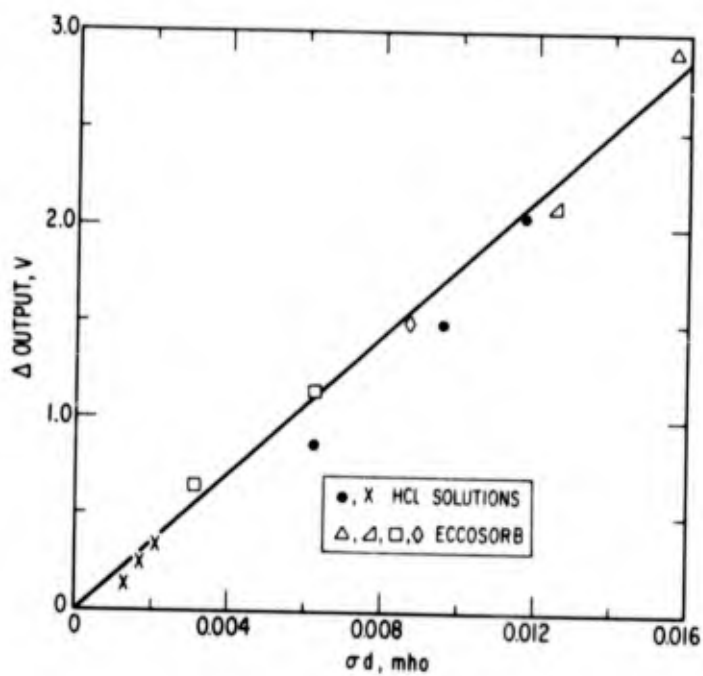
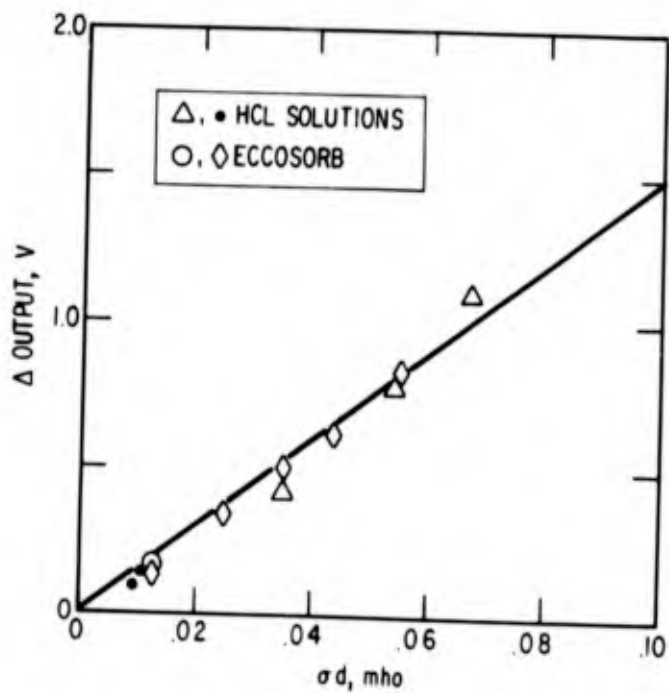


Fig. 10. Calibration Data for High-Gain Channel

Fig. 11. Calibration Data for Low-Gain Channel



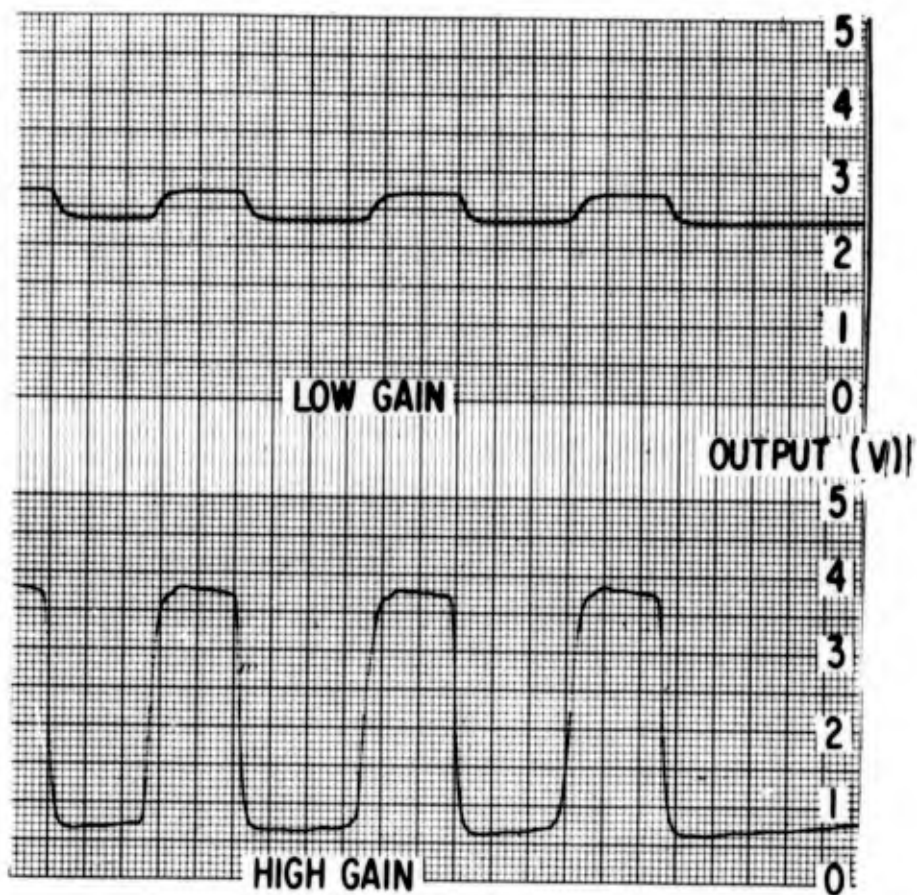


Fig. 12. Recording of High- and Low-Gain Channels During Application and Removal of 0.025 mho Test Fixture (Chart Speed: 1 Large div/sec)

represents the bridge out-of-balance voltage, which is of proper phase to be phase demodulated. Generally $V(t=0) \gg V_o(t)$, but $V(t=0)$ is attenuated by the high pass filter.

Figure 12 also shows that the noise on the high-gain channel is less than 0.1 V.

Figures 10 and 11 show that the sensitivity is linear for a variety of different test fixtures. Sensitivities are approximately 150 V/mho and 15 V/mho for the high- and low-gain channels.

The geometrical factor $W(z')$ is measured with an Eccosorb test fixture. By applying and removing a sheet of 100- Ω /square Eccosorb at various distances from the coil face, the response vs axial separation can be measured.

Figure 13 is a comparison of these data and the expected $W(z')$ determined from Eq. (2) for a bare coil. The data are normalized to unity at $z = 0.5$ in., a distance corresponding to the outside surface of the vehicle.

The measured data decreases with z' more rapidly than does the calculated $W(z')$. This distortion is caused by the ferrite cup, which isolates the coil from the remainder of the instrument structure. Bare coil measurements show good agreement with the calculated $W(z')$ (Ref. 1).

With the data of Fig. 13, the response of the instrument to a thick conducting sample can be calculated. For a sample of thickness d and conductivity σ , the effective value of σd at a point 0.5 in. from the coil face is

$$(\sigma d)_{\text{eff}} = \int_{0.5}^d W(z) dz \quad (4)$$

For these data, the coil radius $r_c = 2$ in. and $z = r_c z'$.

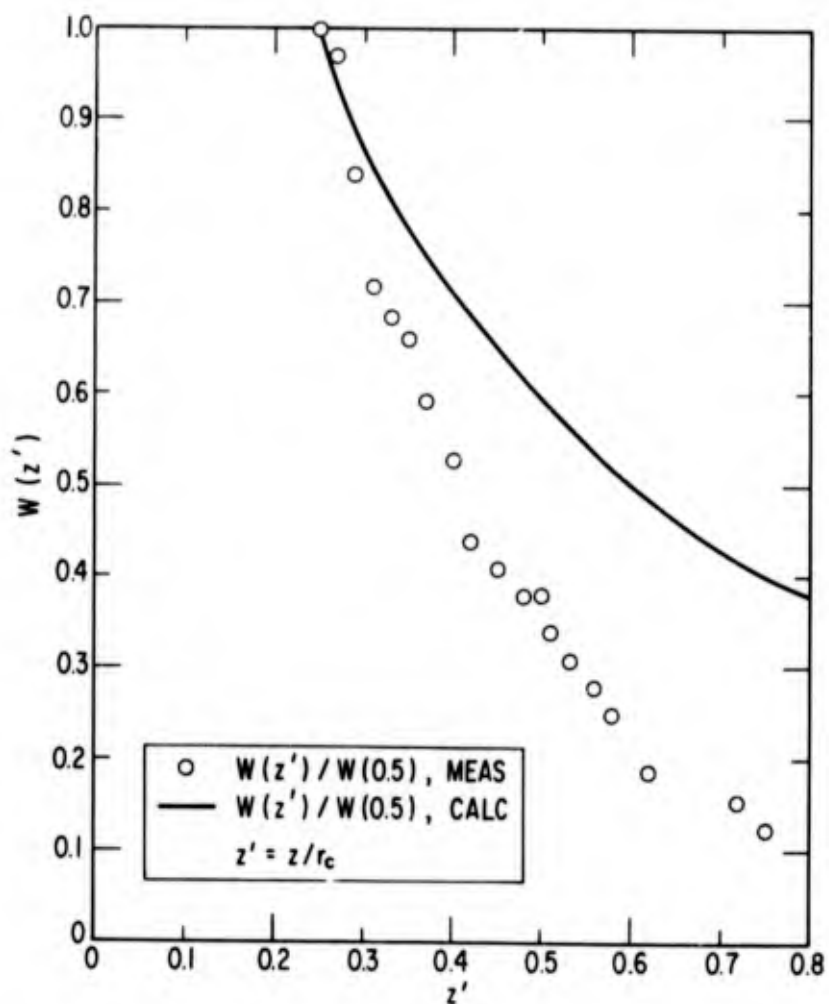


Fig. 13. Geometrical Factor $W(z')$ vs Normalized Axial Separation z (The line is calculated from Eq. (2) for a bare coil. Discrepancy is caused by ferrite cup used for isolation)

Figure 11 includes three data points obtained from 1/4-, 1/2-, and 3/4-in. -thick samples of HCl solution with conductivity of 9.1 mho/m. The effective σ_d calculated from Eq. (4) was 0.077 mho. These data from the HCl solutions are in agreement with the data from the Eccosorb material. This measurement constitutes a check on the validity of the measured geometrical weighting factor $W(z)$.

Figure 10 has data points obtained using 1.65-mho/m and 0.3-mho/m solutions. The sensitivity determined from these data is 6% lower than the 150 V/mho determined from the Eccosorb material. This discrepancy is not significant for the more dilute solutions.

Figure 14 provides the instrument gain vs reference voltage, which is derived from the output of the last stage in the rf amplifier. At a reference voltage of 1.8 V, the gain begins to deviate from unity. At this point the bridge is sufficiently far out of balance that the rf amplifier is beginning to saturate.

At a reference voltage of 2.0 V, the gain becomes indeterminate between the curves labeled "reactive" and "resistive."

The value of the gain depends upon the phase of the out-of-balance signal causing the distortion. If it is from a reactive change in the coil, the gain remains high until the amplifier output is grossly distorted. If the out-of-balance voltage is of the same phase as a resistive change in the coil, the gain falls off more rapidly. The reason for this is that the amplifier has a higher duty cycle when the distorting output is $\frac{\pi}{2}$ rad out of phase with the signal.

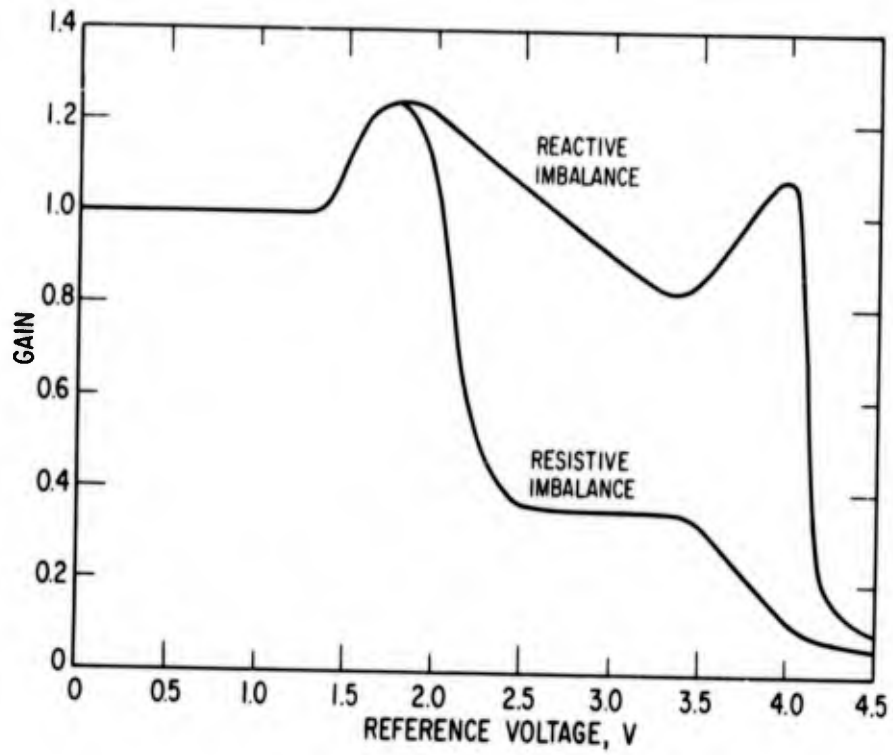


Fig. 14. Instrument Gain vs RF-Amplifier-Output-Monitor Reference Voltage

If another subcommutated or low-sample-rate telemetry channel were available, the phase of the out-of-balance voltage could be telemetered and the gain more accurately determined. Operation of the gauge with the bridge unbalanced to the point of saturating the amplifier is an abnormal situation.

Figure 15 provides thermistor voltage output vs temperature. The solid curve was calculated with a 5000- Ω series limiting resistor and a -4.4% temperature coefficient for the thermistor. The data points are measured values.

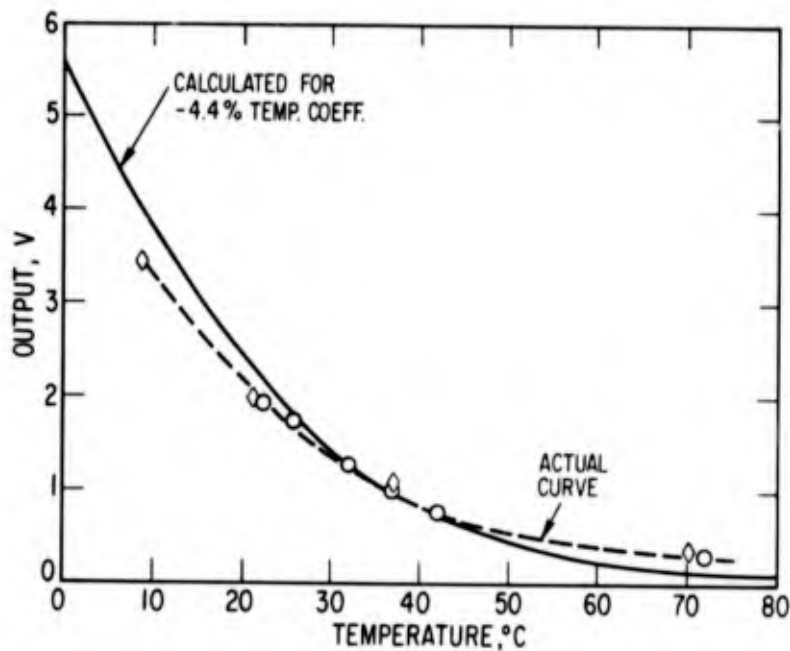


Fig. 15. Temperature-Monitor Voltage vs Temperature

REFERENCES

1. A. E. Fuhs, W. R. Grabowsky, and O. L. Gibb, "Use of Radio Frequency Bridge for Reentry Plasma Diagnostics," J. Spacecraft Rockets 4, 327 (1967).
2. D. M. Dix, Typical Values of Plasma Parameters Around a Conical Reentry Vehicle, TDR-169(3230-22)TN-1, Aerospace Corp. (November 1962).
3. W. P. Thompson, Experimental Evaluation of Flush Electrostatic Probes for Reentry Measurements, TR-0158(3240-20)-4, Aerospace Corp. (July 1967).
4. L. Spitzer, Physics of Fully Ionized Gases, Dover Publications, Inc. New York (1962), p. 110.
5. J. A. Stratton, Electromagnetic Theory, McGraw-Hill Book Co., Inc. New York (1941), p. 263.
6. E. T. Whittaker and G. N. Watson, A Course of Modern Analysis, Cambridge University Press, London (1927), p. 521.
7. F. W. Grover, Inductance Calculations, Dover Publications Inc., New York (1962), p. 110.

UNCLASSIFIED

Security Classification

DOCUMENT CONTROL DATA - R&D		
<i>(Security classification of title, body of abstract and indexing annotation must be entered when the overall report is classified)</i>		
1 ORIGINATING ACTIVITY (Corporate author) Aerospace Corporation El Segundo, California		2a REPORT SECURITY CLASSIFICATION Unclassified
		2b GROUP
3 REPORT TITLE RF BRIDGE ELECTRICAL CONDUCTIVITY GAUGE FOR RMP-B VEHICLE		
4 DESCRIPTIVE NOTES (Type of report and inclusive dates)		
5 AUTHOR(S) (Last name, first name, initial) McPherson, Donald A., Gibb, O. Lloyd, Harbridge, Wallace B., and Fuhs, Allen E.		
6 REPORT DATE June 1968	7a TOTAL NO OF PAGES	7b NO OF REFS 7
8a CONTRACT OR GRANT NO F04695-67-C-0158	9a ORIGINATOR'S REPORT NUMBER(S) TR-0158(3220-20)-2	
b. PROJECT NO.		
c	9b OTHER REPORT NO(S) (Any other numbers that may be assigned this report)	
d	SAMSO-TR-68-238	
10 AVAILABILITY/LIMITATION NOTICES This document is subject to special export controls and each transmittal to foreign governments or foreign nationals may be made only with the prior approval of SAMSO (SMTTA).		
11 SUPPLEMENTARY NOTES	12. SPONSORING MILITARY ACTIVITY Space and Missile Systems Organization Air Force Systems Command Los Angeles, California	
13 ABSTRACT <p>The Reentry Measurements Instrument Package (RMIP) on the Reentry Measurements Vehicle (RMV) is designed to measure properties of the boundary layer and wake for a sharp nosed, slender body. One of the experimental instruments is an rf bridge that measures the dc conductivity of the plasma sheath formed about the vehicle. Because conductivity is directly proportional to electron density, knowledge of the electron-neutral collision frequency is sufficient to determine the electron density from the conductivity. For the RMP-B vehicle, it is expected that the conductivity will be in the range 0.3 to 1.0 mho/m for a refrasil heat shield with 50 ppm Na or equivalent contaminants. The conductivity meter was designed with a dynamic range of 0.1 to 10.0 mho/m. The system study providing design criteria is reviewed. Detailed operational information on instrument performance is presented.</p>		

DD FORM 1473
(IFACSIMILE)

UNCLASSIFIED

Security Classification

Boundary Layer Electron Density
Conductivity Gauge
Reentry Communications
RF Bridge
RMP-B

Abstract (Continued)